Signatures of quasi-Dirac neutrinos in diffuse high-energy astrophysical neutrino data

[arXiv:2503.19960]

Yago Porto
UFABC (Brazil)
*On the move to TU Munich

UFABC

FAPESP
FUNDAÇÃO DE AMPARO À PESQUISA DO ESTADO DE SÃO PAULO

Collaboration with C. Arguelles, K. Carloni, B. Dev and S. Jana

CETUP*2025 (July 11, 2025)

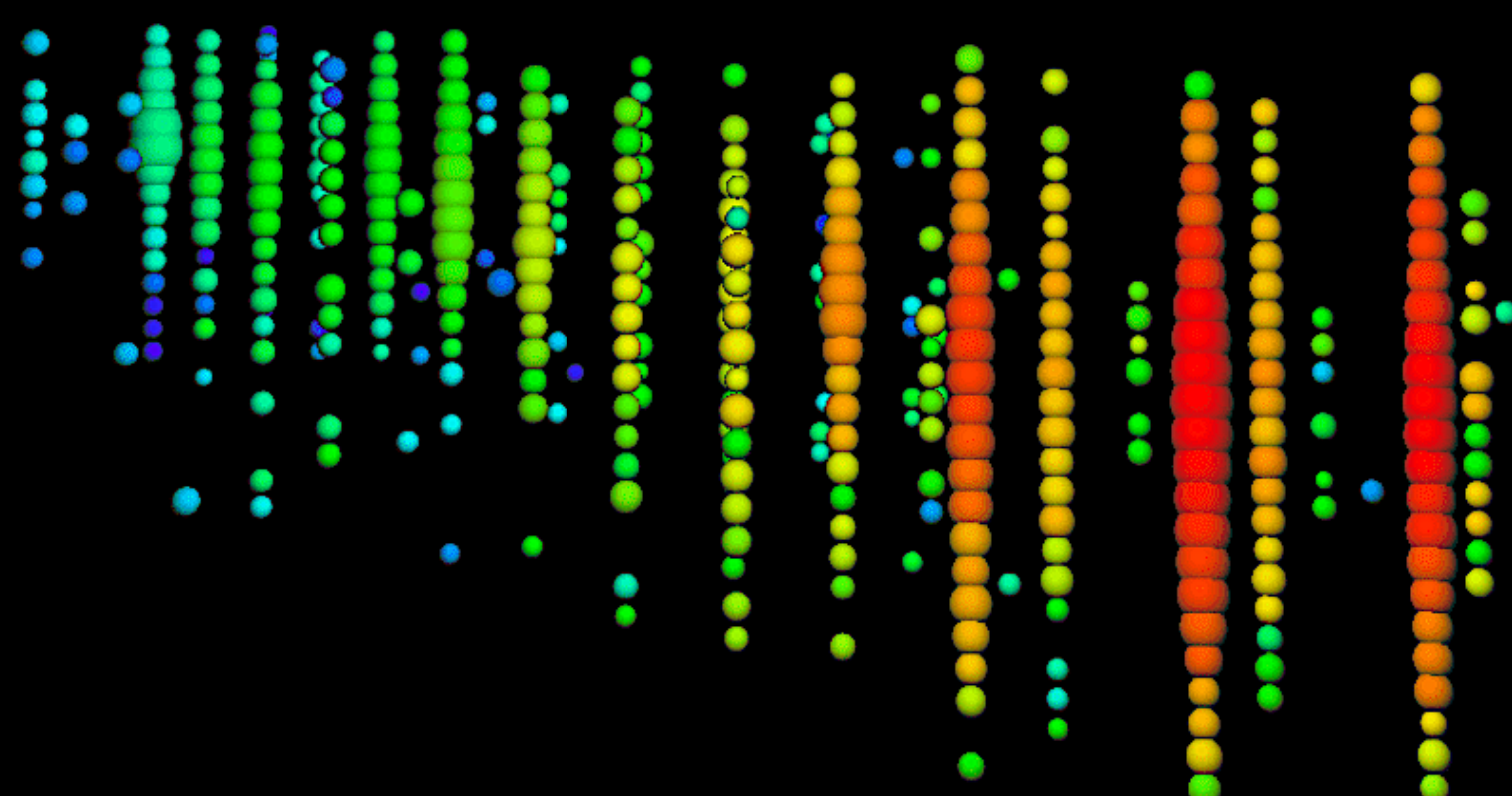

Overview

We search for signatures of extremely long-baseline oscillations between left- and right-handed neutrinos using the high-energy astrophysical neutrino spectra measured by IceCube.

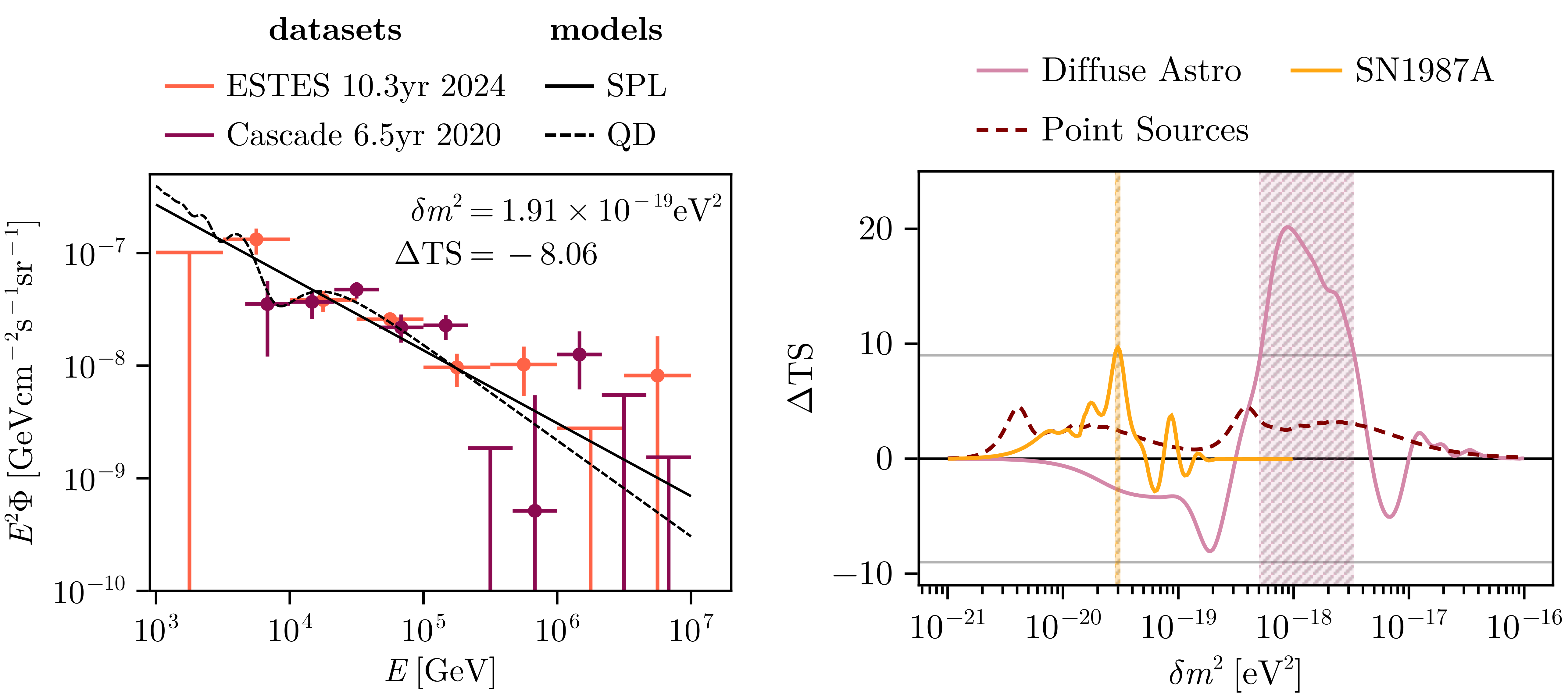

- Assuming a single power law (SPL) astrophysical flux and source distribution following the star formation rate.

Overview

We search for signatures of extremely long-baseline oscillations between left- and right-handed neutrinos using the high-energy astrophysical neutrino spectra measured by IceCube.

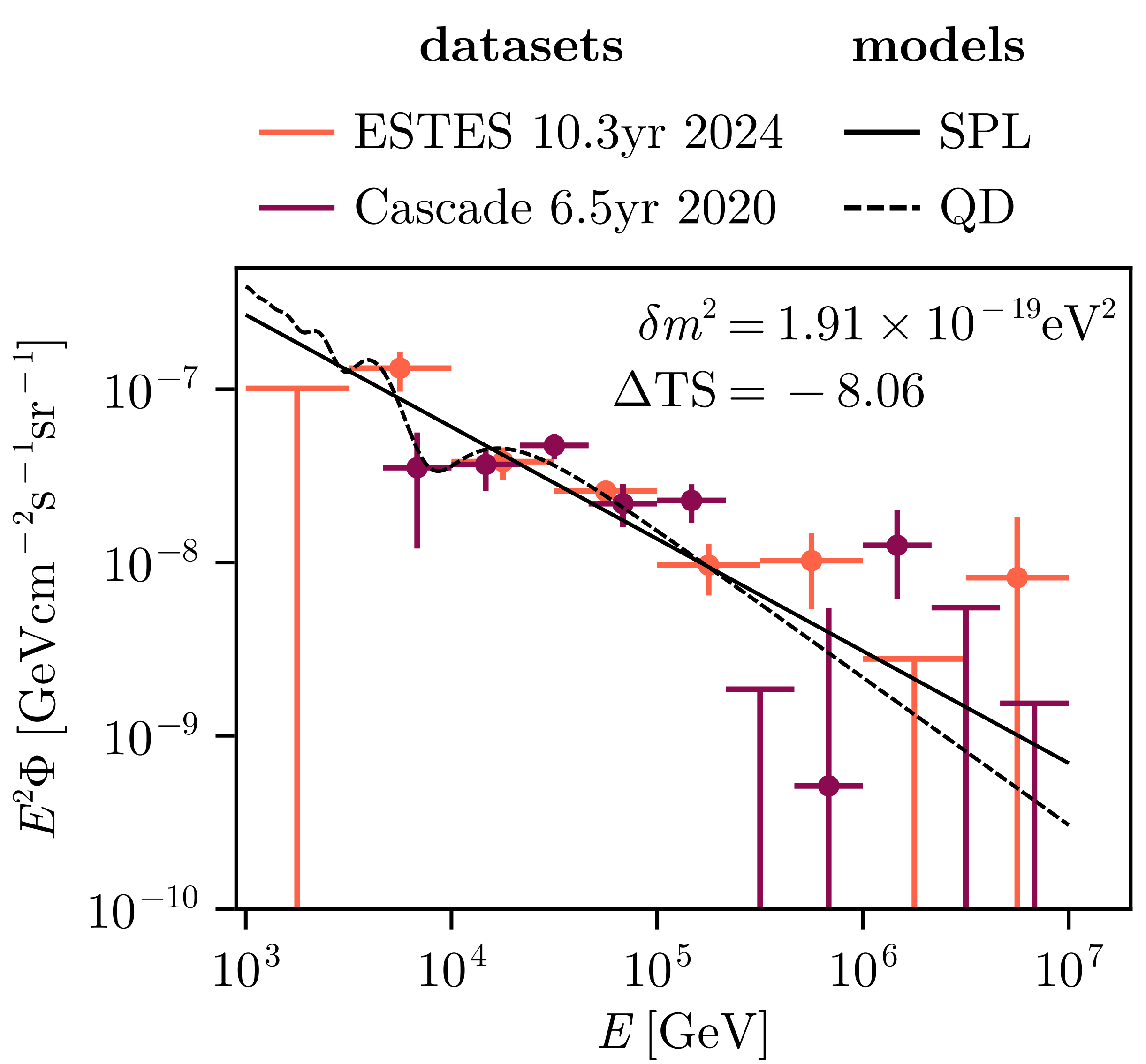

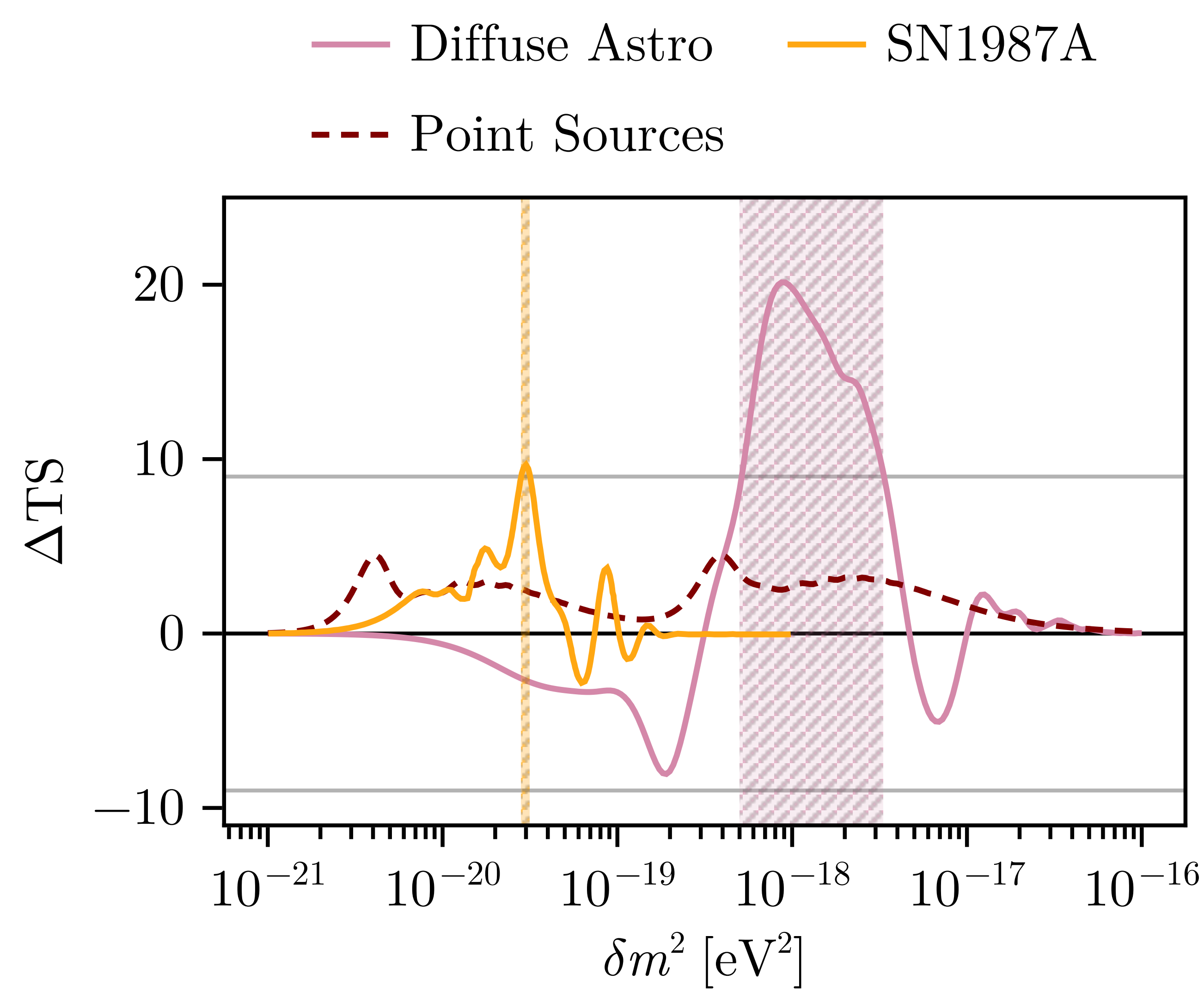

- $\delta m^2 = [5 \times 10^{-19}, 3 \times 10^{-18}]$ eV^2 disfavored at the 3σ level.
- Preference for $\delta m^2 = 1.9 \times 10^{-19}$ eV^2 at 2.8σ level driven by the low energy bins.

Outline

- Discovery of high-energy (HE) astrophysical neutrinos in IceCube.
- Overview of the different ways IceCube measures the diffuse neutrino flux.
- Description of the mild but persistent tension among these datasets.
- Discussion of quasi-Dirac neutrinos and their astrophysical signatures.
- The impact of the chosen source distribution on the results.

Astrophysical neutrinos at IceCube

Discovery of High-Energy Astrophysical Neutrinos (2013)

- First detection of two events with energies around 1 PeV [IceCube Collab., PRL 111, 021103 (2013).]
- Detection of 28 events with energies from 60 TeV to 1 PeV [IceCube Collab., Science 342, 1242856 (2013).]

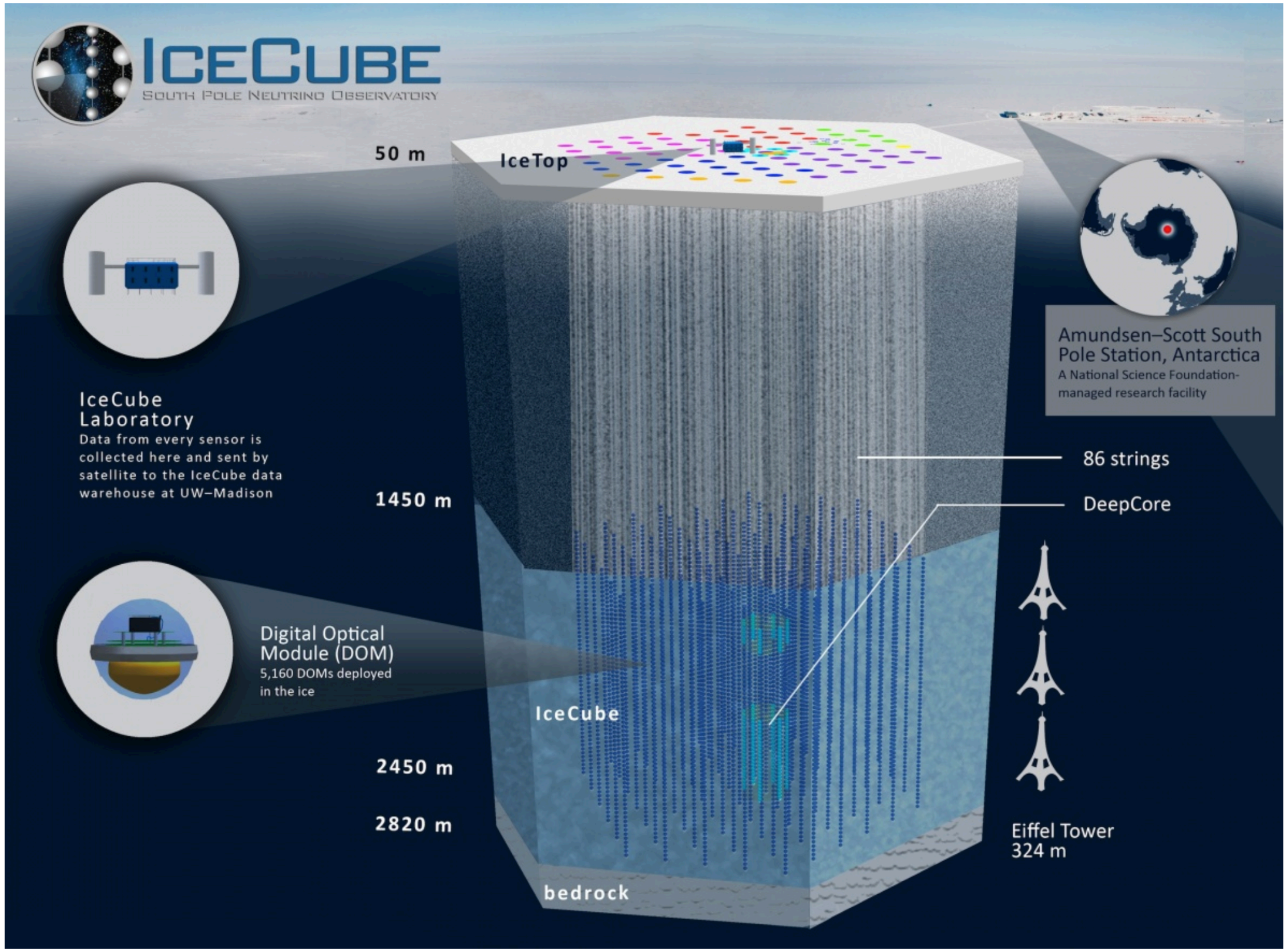

Figure: Schematic of the IceCube Neutrino Observatory at the South Pole, illustrating DOM string layout and detector depth.

Discovery of High-Energy Astrophysical Neutrinos (2013)

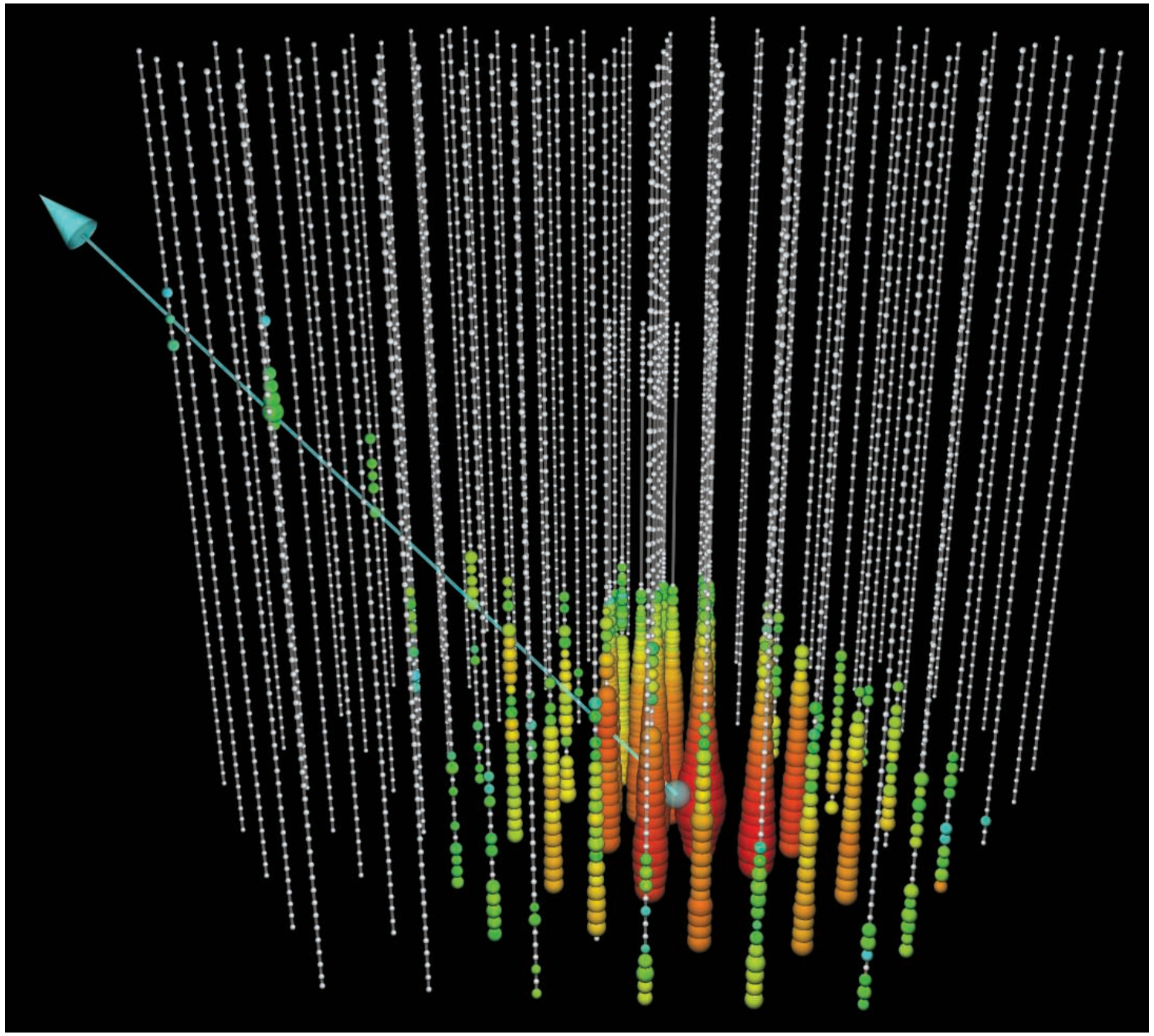

250 TeV Track Event in IceCube

At the neutrino interaction point (bottom), a large particle shower is visible, with a muon produced in the interaction leaving up and to the left. The direction of the muon indicates the direction of the original neutrino.

Detection Topologies in IceCube

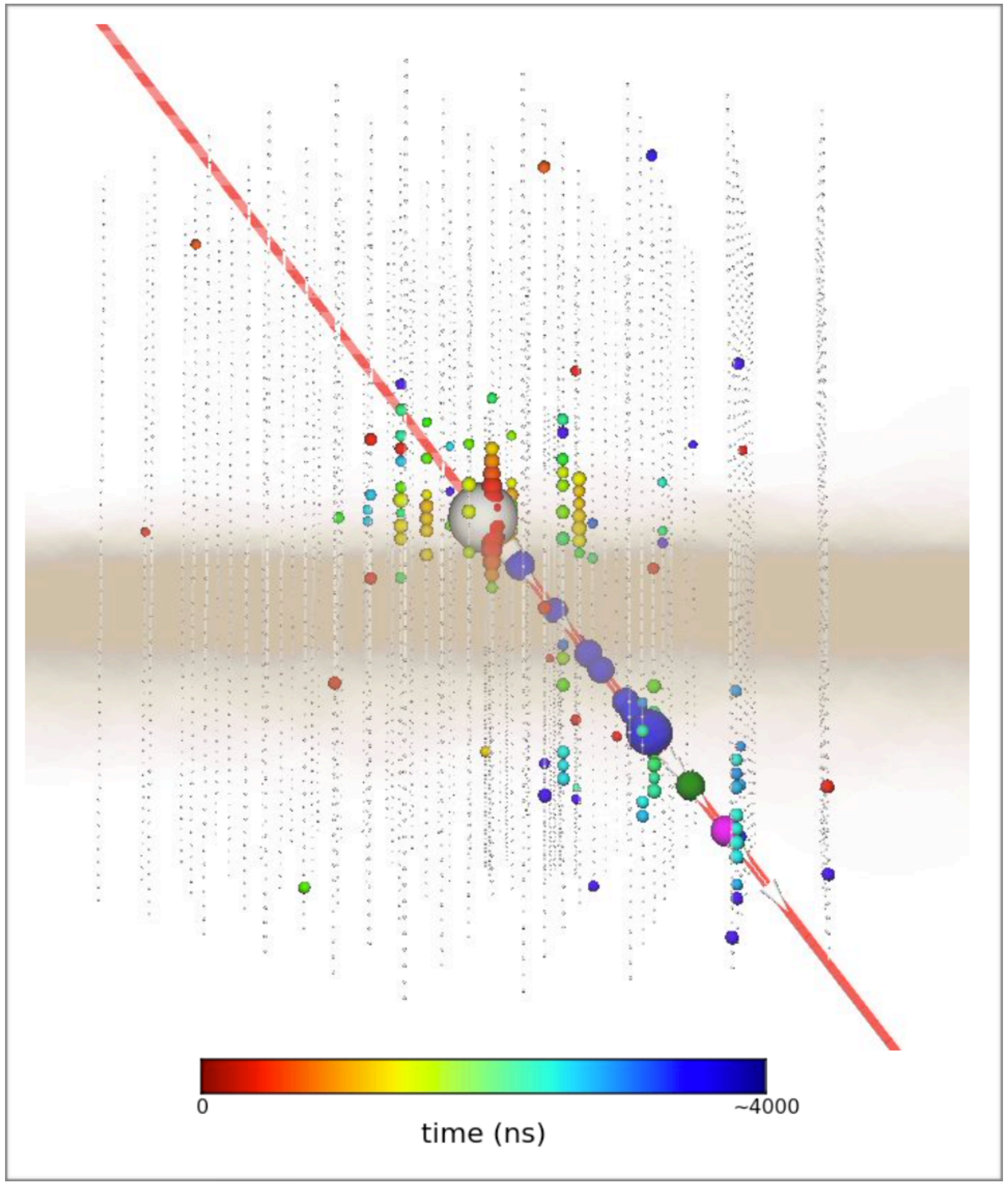

Tracks
(CC ν_μ interactions)
Superior angular resolution

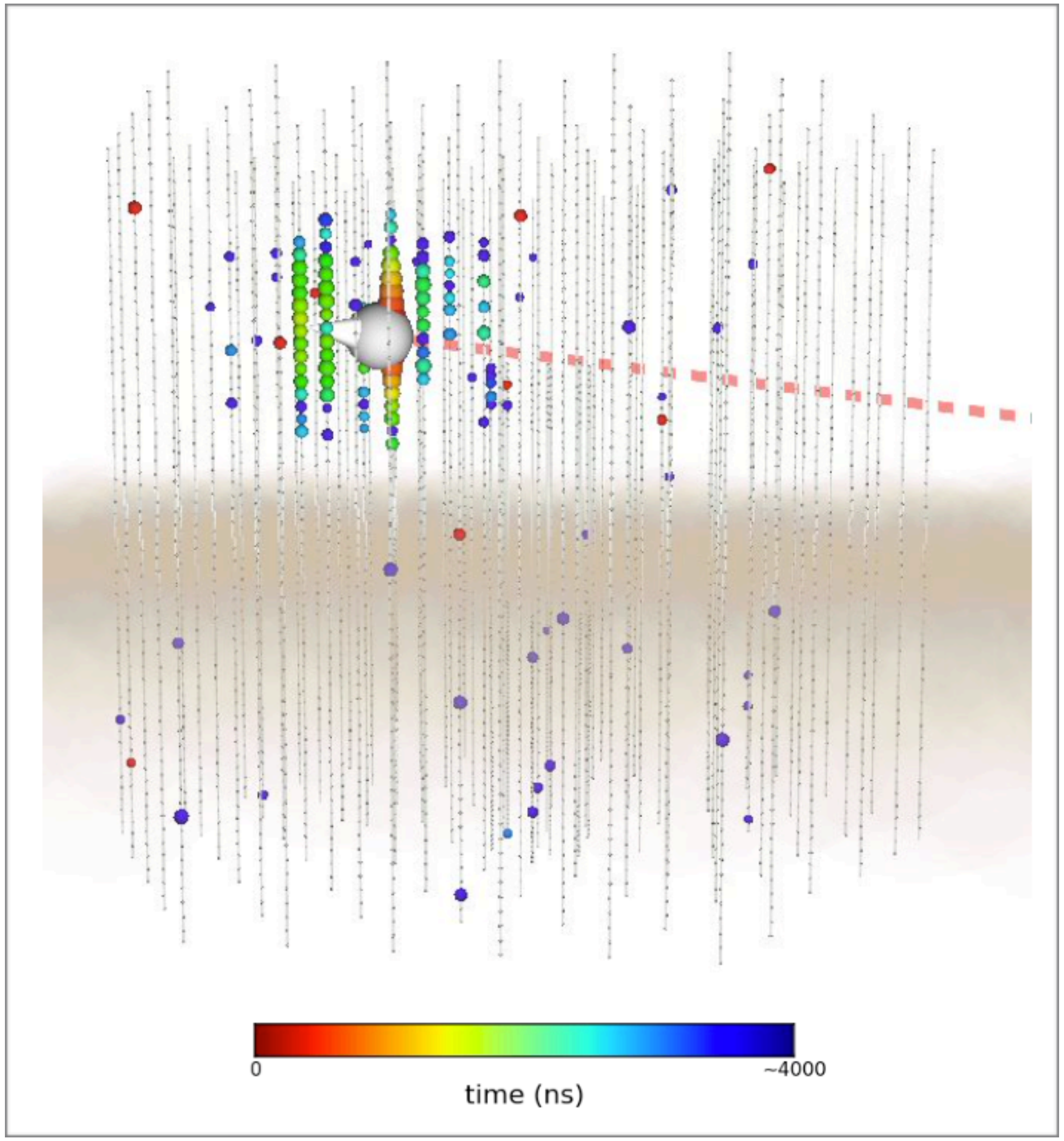

Cascades
(CC ν_e/ν_τ and all NC interactions)
Superior energy resolution

Sarah Mancina (Thesis, UW-Madinson, 2022)

Sources of HE Astrophysical Neutrinos

- No strong anisotropy has been observed in the diffuse HE neutrino flux.
- A first candidate source (TXS 0506+056) was identified in 2017, following a multi-messenger campaign that linked a single IceCube event to γ-rays.
- A retrospective analysis of IceCube data revealed a neutrino burst (19 events) from TXS 0506+056 in 2014–2015.
- The most significant source detected to date (4.2σ) is NGC 1068, a steady emitter associated with ~79 events.

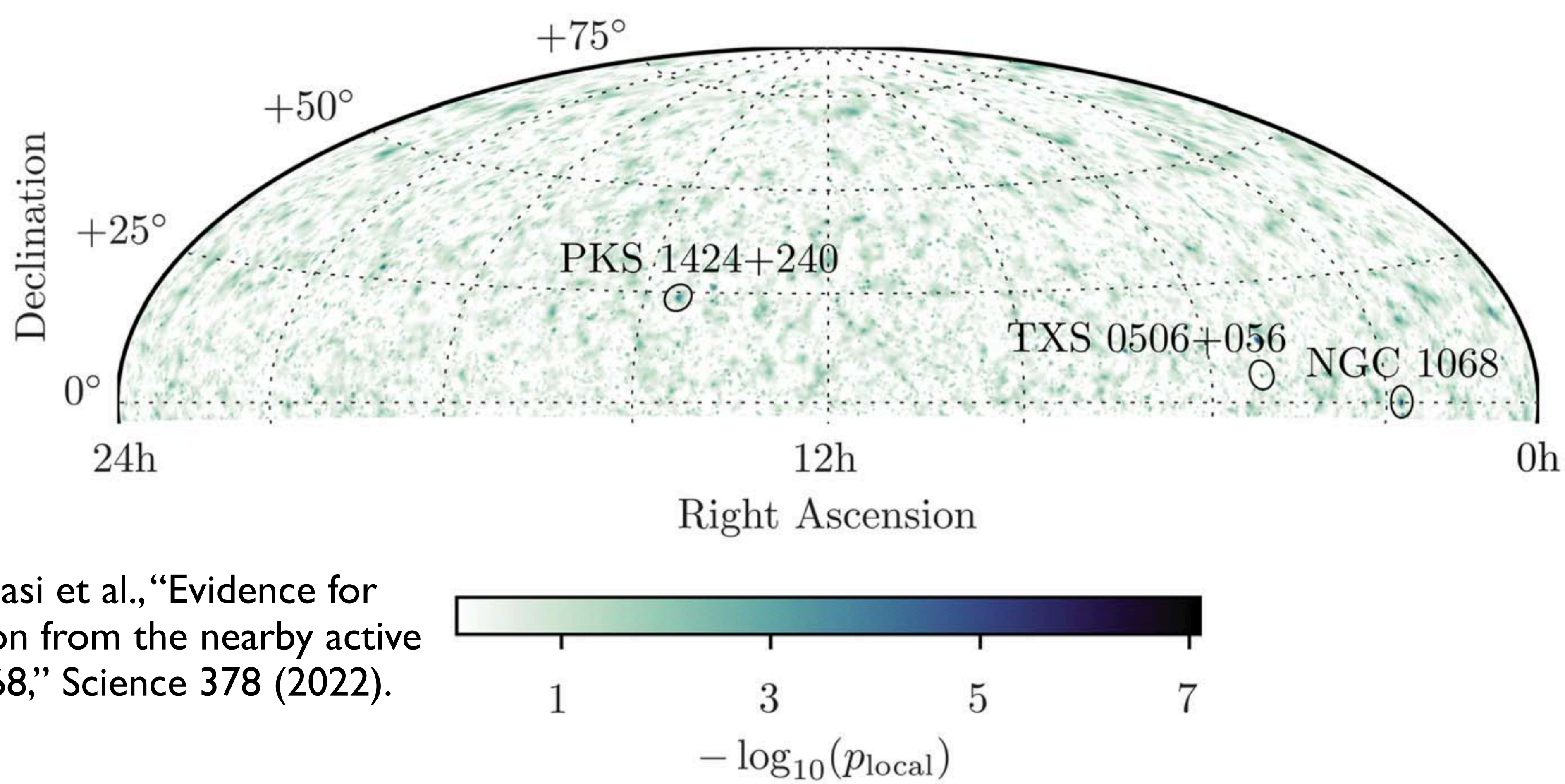

IceCube , R. Abbasi et al., "Evidence for neutrino emission from the nearby active galaxy NGC 1068," Science 378 (2022).

Overview of the main IceCube datasets

High Energy Starting Events (HESE)

- HE neutrinos were first observed via starting events, where the **interaction vertex is contained within the fiducial volume**. These events span all neutrino flavors and arrive from all directions above 60 TeV.
- The HESE flux well described by a SPL spectrum. Alternative parameterizations do not provide a significant improvement over the SPL.

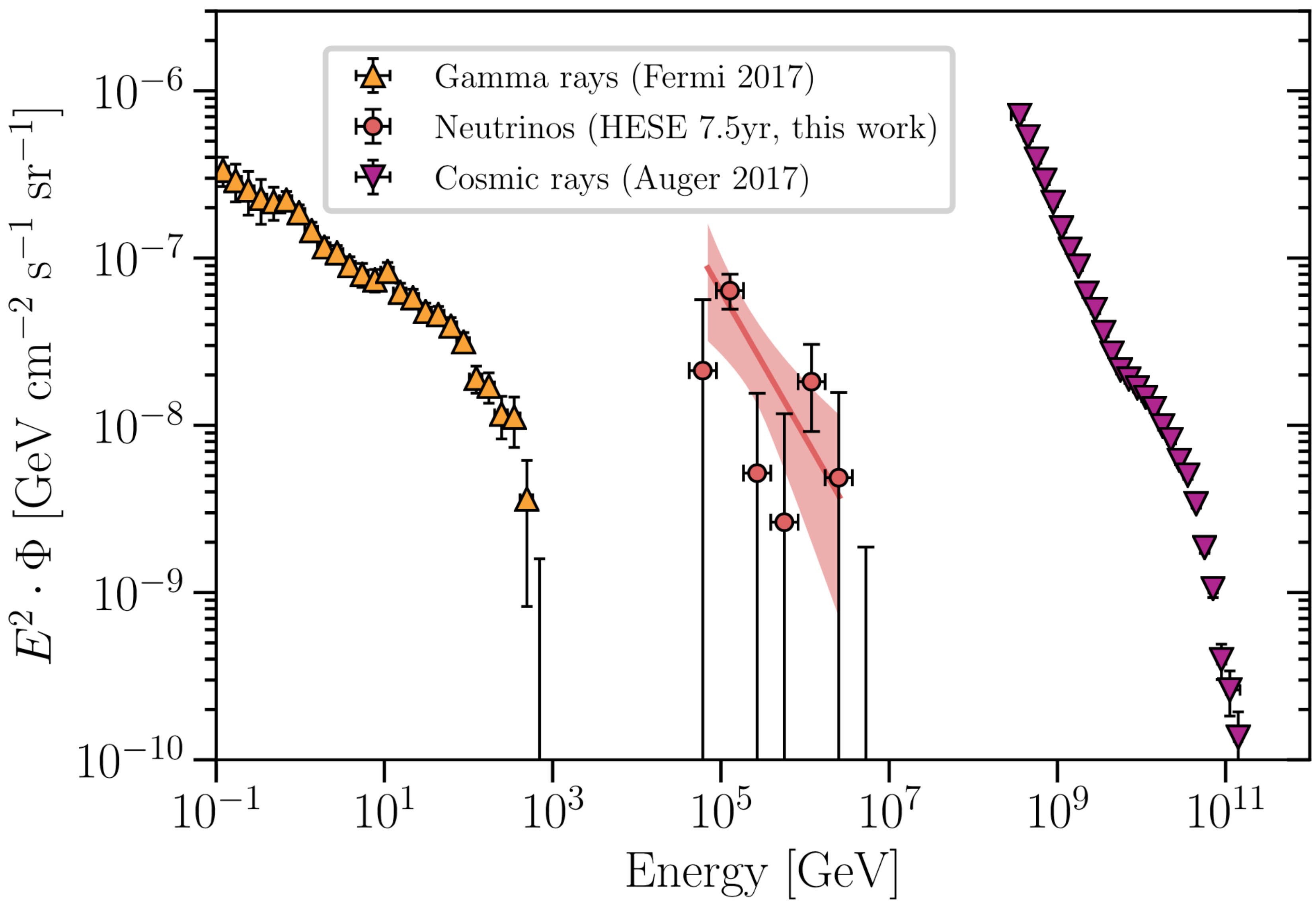

IceCube Collaboration, PRD 104 (2021) 022002

SPL (in red)

$$\Phi = \Phi_0 \left(\frac{E_\nu}{100\ \mathrm{TeV}} \right)^{-\gamma} \times 10^{-18}\ \mathrm{GeV}^{-1}\ \mathrm{cm}^{-2}\ \mathrm{s}^{-1}\ \mathrm{sr}^{-1}$$

with $\gamma = 2.87^{+0.20}_{-0.19}$

High Energy Starting Events (HESE)

IceCube Collaboration, PRD 104 (2021) 022002

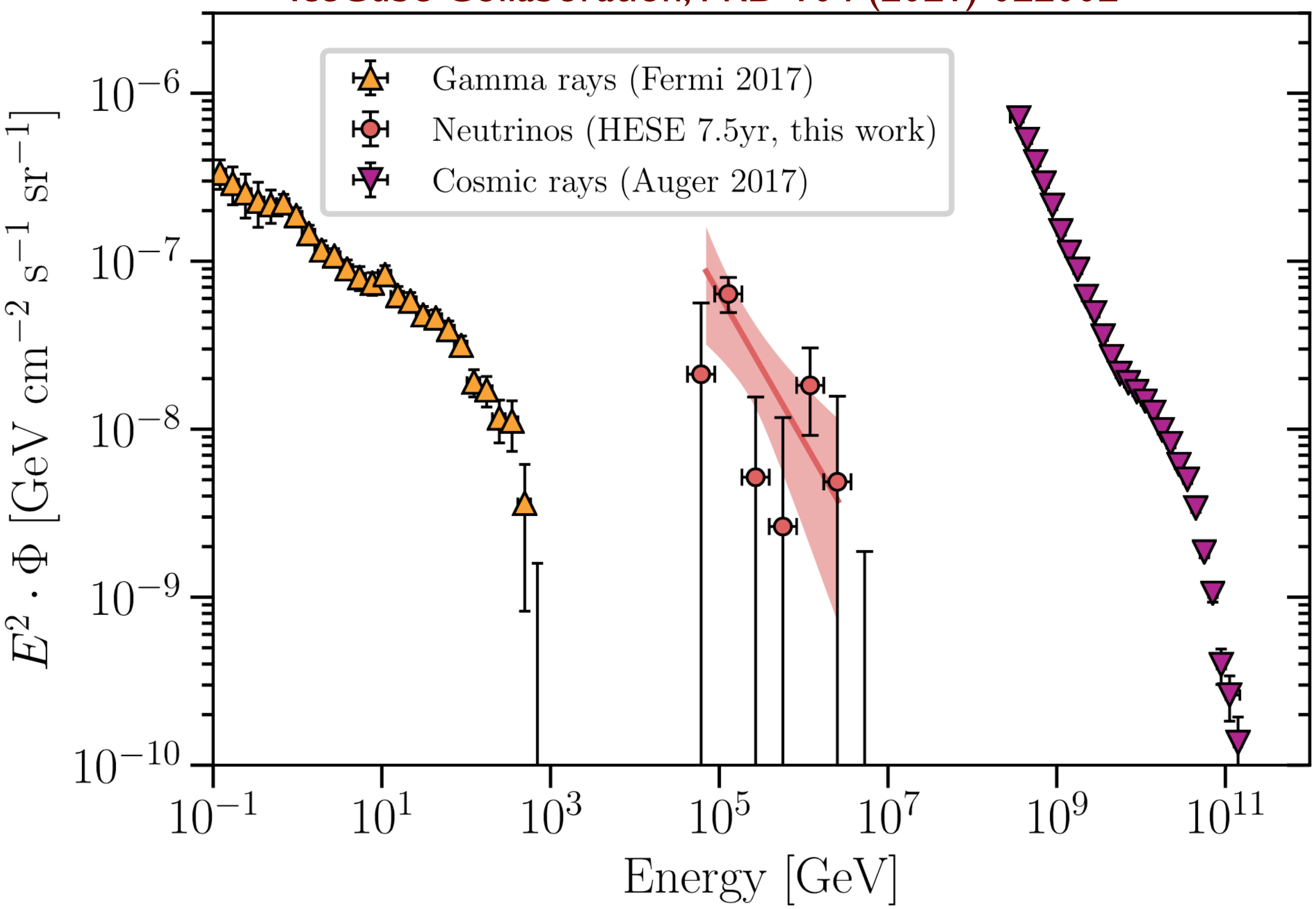

SPL (in red)

$$\Phi = \Phi_0 \left(\frac{E_\nu}{100\,\mathrm{TeV}} \right)^{-\gamma} \times 10^{-18}\,\mathrm{GeV}^{-1}\,\mathrm{cm}^{-2}\,\mathrm{s}^{-1}\,\mathrm{sr}^{-1}$$

with $\gamma = 2.87^{+0.20}_{-0.19}$

- The geometric acceptance is nearly isotropic, but **background rejection is better in the Southern sky:** atmospheric ν's arriving from above are often accompanied by muons that trigger the veto.
- Best fit spectral index changed from $\gamma_{\mathrm{astro}} = 2.3^{+0.3}_{-0.3}$ **(2014)** to $\gamma_{\mathrm{astro}} = 2.87^{+0.20}_{-0.19}$ **(2020)**, driven by more low-energy events in the last 4.5 years.

Medium Energy Starting Events (MESE)

- However, when extending to lower energies, potential deviations from the power-law spectrum appear at ~30 TeV.
- This excess is observed in the down-going component of the data (southern sky).
- Since IceCube has strong control over down-going atmospheric backgrounds, this excess is likely of astrophysical origin.
- Atmospheric neutrinos are vetoed via their coincidence with muons, while atmospheric muons are rejected because they originate outside the detector volume (i.e., they are not starting events).

IceCube Collaboration, PRD 91 (2015) 022001

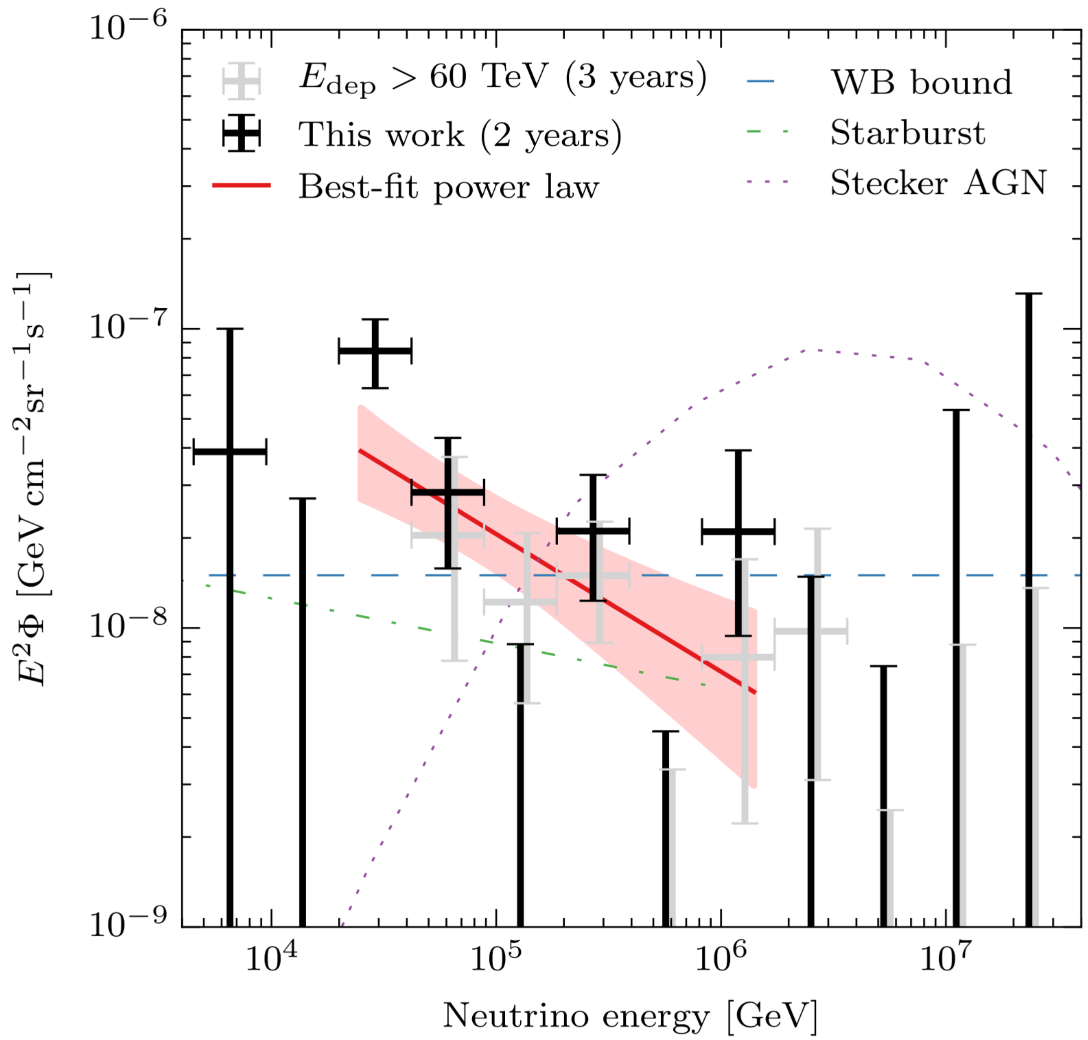

SPL with $\gamma = 2.46 \pm 0.12$ (in red)

Medium Energy Starting Events (MESE)

- The excess around 30 TeV is primarily seen in down-going events from the southern sky.

IceCube Collaboration, PRD 91 (2015) 022001

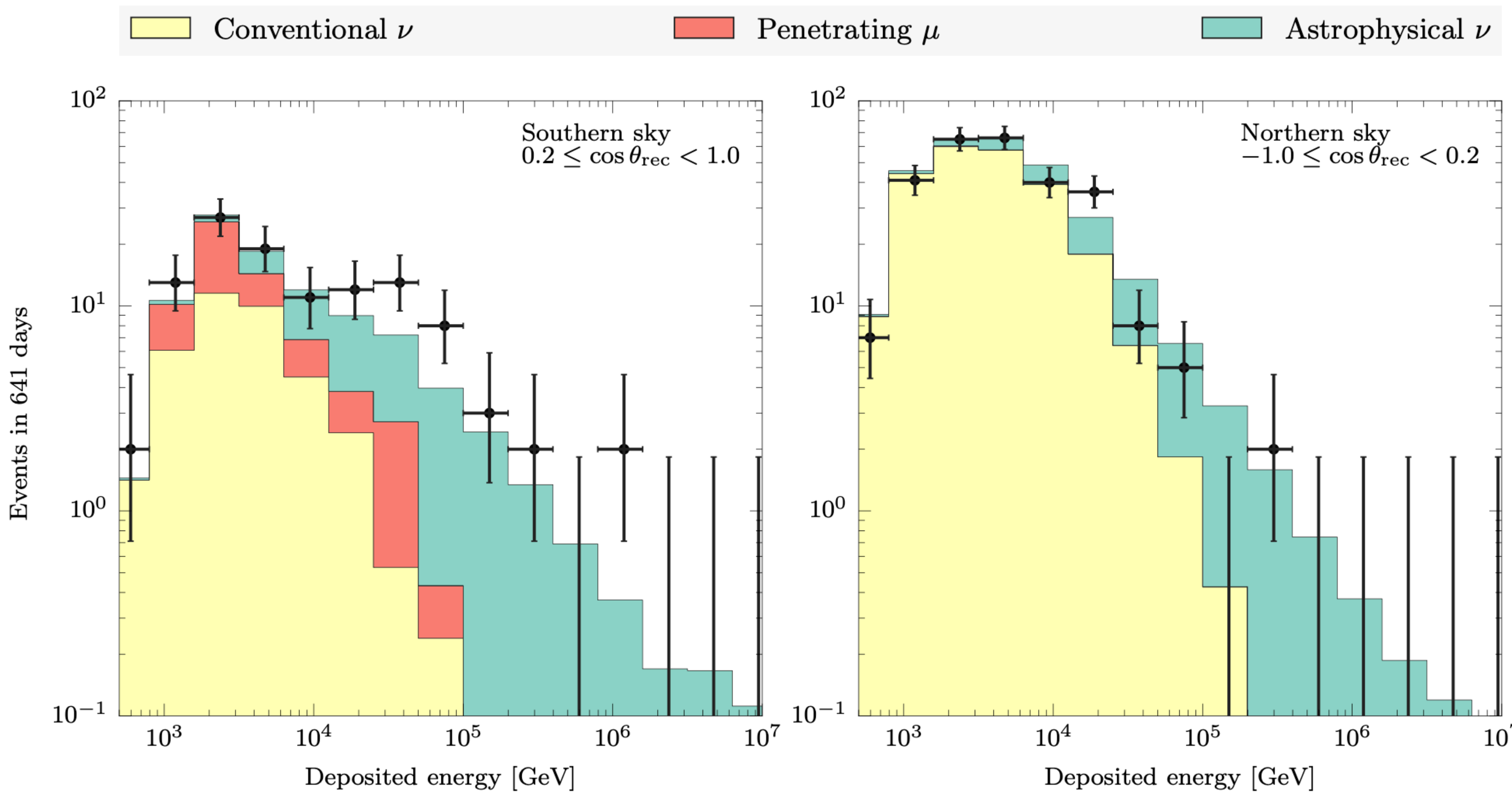

- Updated MESE analysis is in preparation [*PoS* ICRC2023 (2023) 1007]

Cascades

- This departure from the SPL is primarily driven by cascade-like events.
- The cascades dataset selects events whose cascades start inside the detector's fiducial volume (southern hemisphere neutrinos dominate the sensitivity).
- The cascades sample is also consistent with MESE's departures from the SPL.
- A broken power law (BPL) provides a better fit, with a harder spectrum for E<30 TeV and a softer spectrum for E>30 TeV. Significant deviations from the SPL appear at energies above hundreds of TeV.

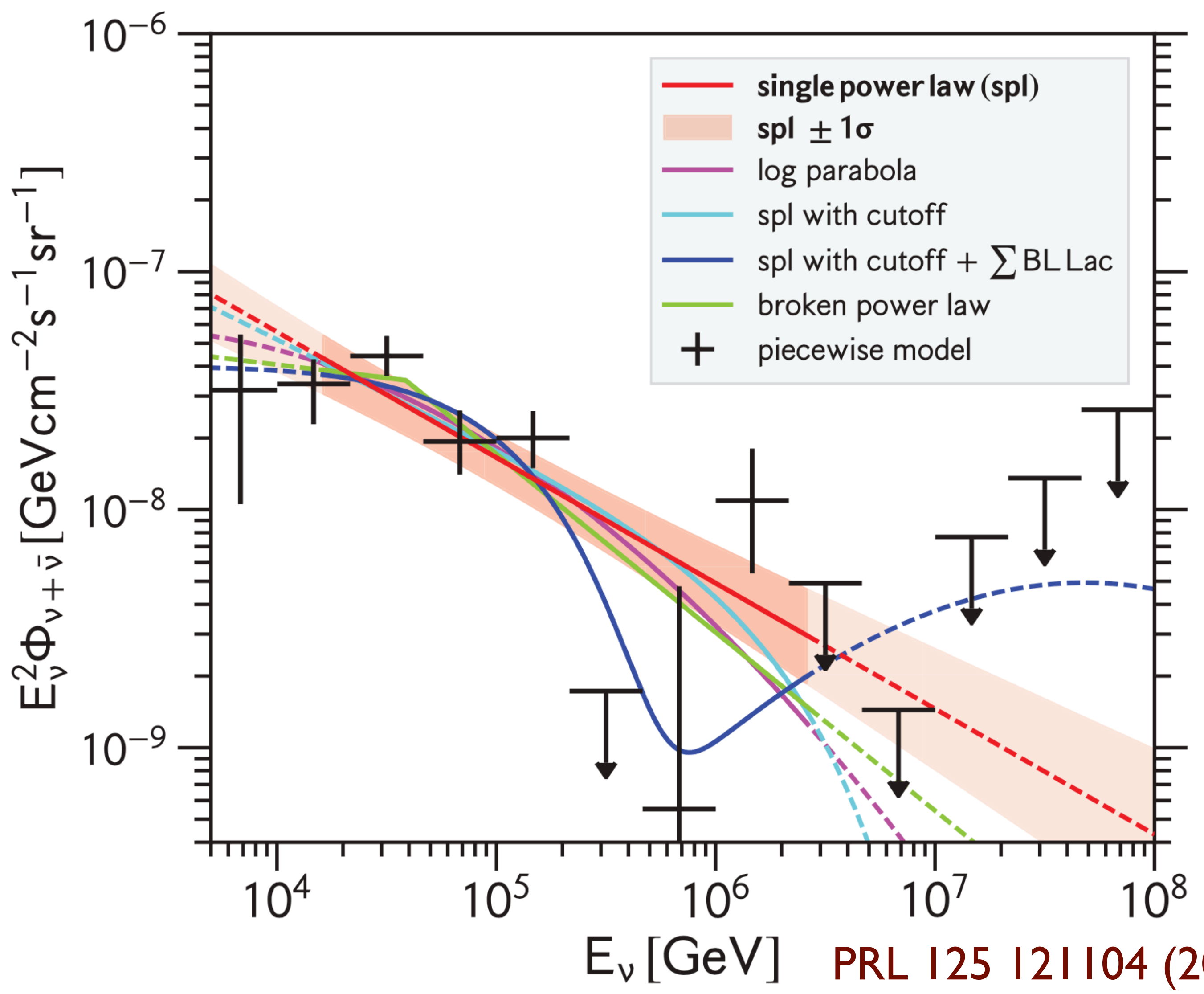

PRL 125 121104 (2020)

SPL (red) with $\gamma = 2.53 \pm 0.07$

Broken Power Law (BPL) in green

$$\Phi(E) = \begin{cases} \Phi_b \left(\frac{E}{E_b}\right)^{-\gamma_1}, & E \leq E_b, \\ \Phi_b \left(\frac{E}{E_b}\right)^{-\gamma_2}, & E > E_b. \end{cases}$$

with $\log_{10}(E_b/\text{GeV}) = 4.6^{+0.5}_{-0.2}$

$$\gamma_1 = 2.11^{+0.29}_{-0.67}$$

$$\gamma_2 = 2.75^{+0.29}_{-0.14}$$

Enhanced Starting Track Event Selection (ESTES).

- By vetoing atmospheric neutrinos and muons produced outside the detector (and machine learning) ESTES can probe lower-energy regions that are heavily background-dominated.
- Since ESTES events originate within the detector, they achieve an energy resolution comparable to cascades.
- However, the spectral features of ESTES show mild tension with cascades, as it favors a larger spectral index below 30 TeV.

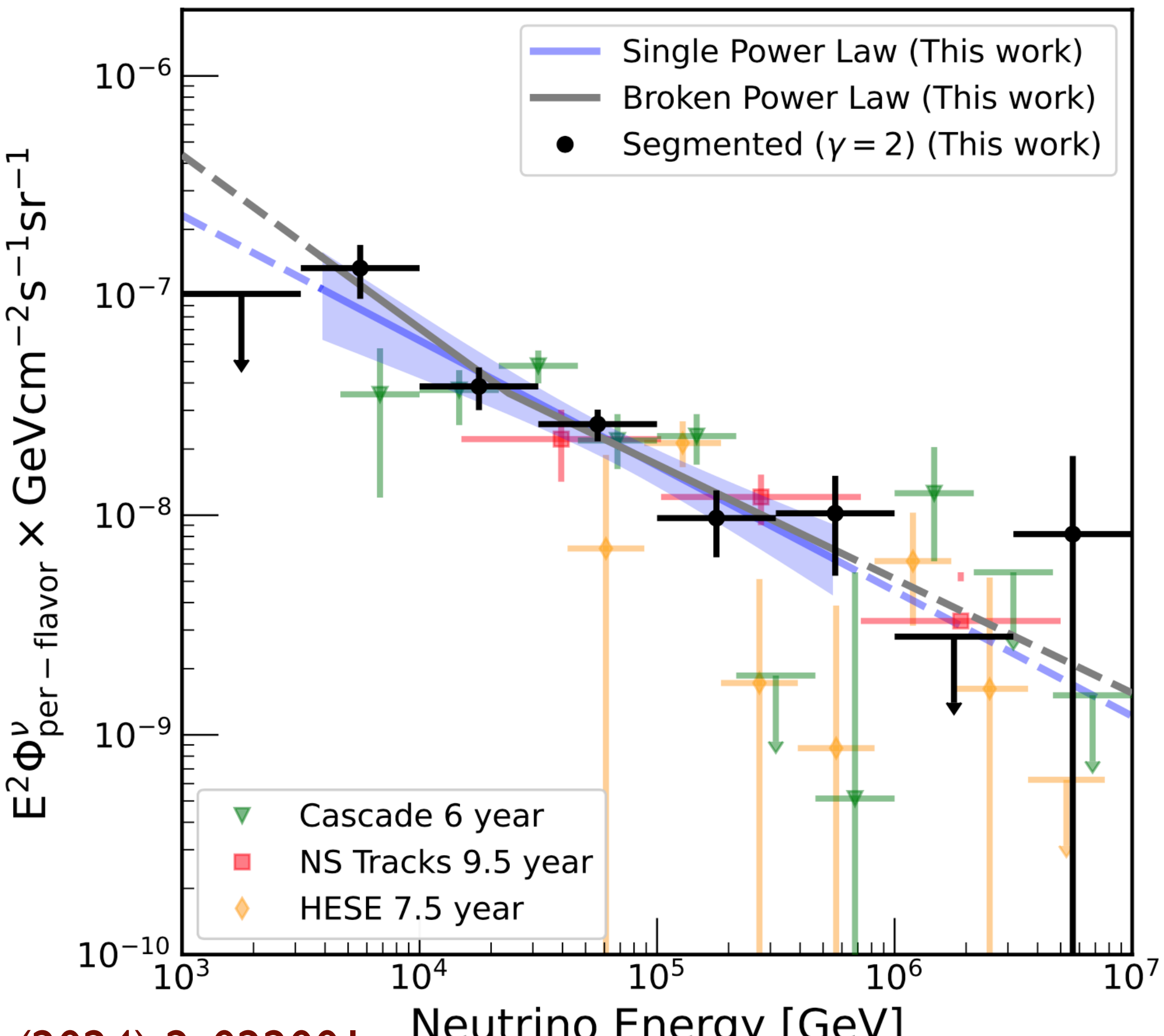

SPL (blue) with $\gamma = 2.58^{+0.10}_{-0.09}$

Broken Power Law (BPL) in grey

$$\Phi(E) = \begin{cases} \Phi_b \left(\frac{E}{E_b}\right)^{-\gamma_1}, & E \le E_b, \\ \Phi_b \left(\frac{E}{E_b}\right)^{-\gamma_2}, & E > E_b. \end{cases}$$

with $\log_{10}(E_b/\text{GeV}) \sim 4.36$

$$\gamma_1 = 2.79^{+0.30}_{-0.50}$$
$$\gamma_2 = 2.52^{+0.10}_{-0.09}$$

PRD 110 (2024) 2, 022001

Quasi-Dirac neutrinos in the astrophysical regime

Neutrino masses

- Neutrinos are massless in the Standard Model (SM):
  - The content of the SM (Q, u^c, d^c, L, e^c, H) contains no right-handed partners ν^c and, therefore, no Dirac mass terms $m_D \nu \nu^c$.
  - Imposing a Majorana mass term of the type $m_M \nu \nu$ breaks $SU(2)_L$-gauge invariance.
  - SM preserves $B - L$.
  - Gravitational effects contribute at most $\sim 10^{-5}$ eV, much smaller than the mass scales set by the neutrino mass splittings ($\sqrt{\Delta m^2_{21}} \sim 10^{-2}$ eV and $\sqrt{\Delta m^2_{31}} \sim 10^{-1}$ eV).
- **Simplest solution:** add SM-singlet right-handed neutrinos (ν^c), allowing both Dirac and Majorana mass terms, $M \nu^c \nu^c$.

$$M_\nu = \begin{pmatrix} 0 & m_D \\ m_D & M \end{pmatrix}$$

Neutrino nature and oscillation phenomenology

$$M_\nu = \begin{pmatrix} 0 & m_D \\ m_D & M \end{pmatrix}$$

- Dirac neutrinos ($M = 0$)
  - Physical eigenstates are linear combinations of ν and ν^c with maximal mixing.
  - Both eigenstates have the same mass m_D.
  - A purely left-handed neutrino ν is not an eigenstate and it could, in principle, oscillate ($\nu \leftrightarrow \nu^c$).
  - However, since the masses are degenerate, no phase difference accumulates, and no oscillation occurs.
- Seesaw Majorana neutrinos ($M \gg m_D$)

  [Minkowski (PLB '77); Mohapatra, Senjanovic (PRL '80); Yanagida '79; Gell-Mann, Ramond, Slansky '79]
  - Physical eigenstates are (to a good approximation) ν and ν^c themselves.
  - The active ν has mass m_D^2/M and ν^c has mass M.
  - The produced left-handed neutrino ν cannot oscillate.
- Therefore, neither Dirac nor seesaw Majorana neutrinos give rise to additional oscillations (albeit for entirely different reasons).

Neutrino nature and oscillation phenomenology

- Quasi-Dirac neutrinos ($M \ll m_D$)

  [Wolfenstein (NPB '81); Petcov (PLB '82); Valle, Singer (PRD '83); Kobayashi, Lim (PRD '01)]

  - Physical eigenstates are linear combinations of ν and ν^c with ***near*** maximal mixing.
  - The eigenstates have masses $m_D \pm \frac{M}{2}$.
  - Oscillation frequency is proportional to $\delta m^2 = 2m_D M$, which can be many orders of magnitude smaller than the usual scales $\Delta m^2_{21} = 7.5 \times 10^{-5}$ eV^2 and $\Delta m^2_{31} = 2.5 \times 10^{-3}$ eV^2.

Quasi-Dirac oscillations

- QD neutrinos are fundamentally Majorana fermions but mimic Dirac behavior in laboratory experiments due to their extremely small mass-squared splittings.

- Constraints from solar neutrino data:
  $\delta m^2_{1,2} \lesssim 10^{-12}$ eV^2

(de Gouvea, Huang, Jenkins, 0906.1611; Ansarifard, Farzan, 2211.09105)

- From laboratory searches:
  $\delta m^2_3 \lesssim 10^{-5}$ eV^2

- Quasi-Dirac oscillations in astrophysical scales:

$$P_{\alpha\beta} = \frac{1}{2}\sum_{k=1}^{3}\left|U^*_{\beta k}U_{\alpha k}\right|^2\left[1+\cos\left(\frac{\delta m_k^2 L_{\rm eff}}{2E}\right)\right]$$

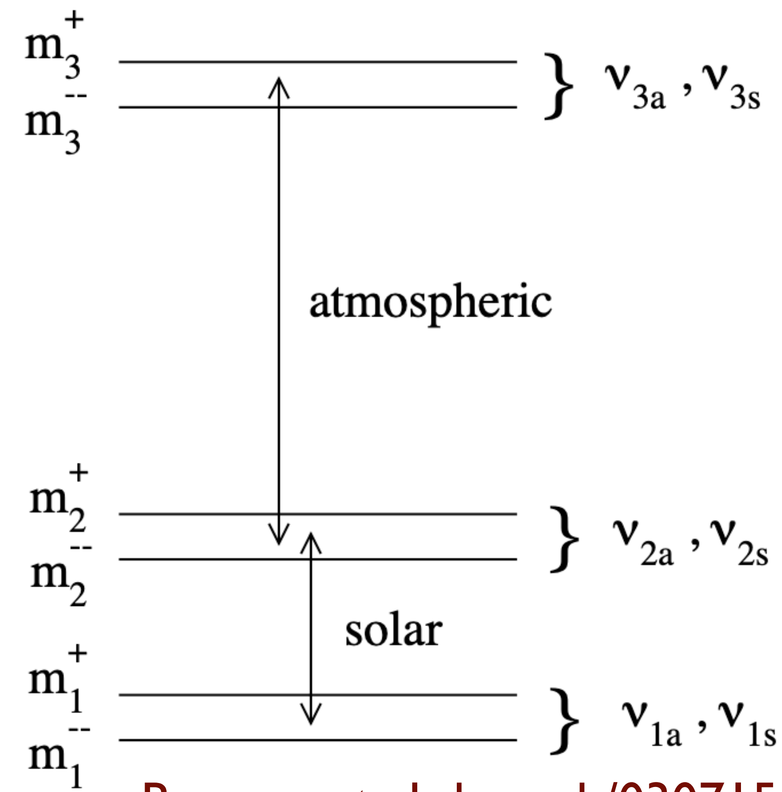

Beacom et al., hep-ph/0307151 (PRL '04)

$$L_{\rm eff} = \int \frac{dz}{H(z)(1+z)^2} \qquad H(z) = H_0\sqrt{\Omega_m(1+z)^3 + \Omega_\Lambda + \left(1-\Omega_m-\Omega_\Lambda\right)(1+z)^2}$$

- Both theoretical and phenomenological aspects have been extensively studied in the literature.

The distribution of neutrino sources

Neutrino sources

- The sources of most diffuse astrophysical neutrino flux remain unknown, but they are likely distributed across all cosmological times and distances.
- We first assume their distribution follows the star formation rate density (SFRD), so the number of sources in a comoving volume element is

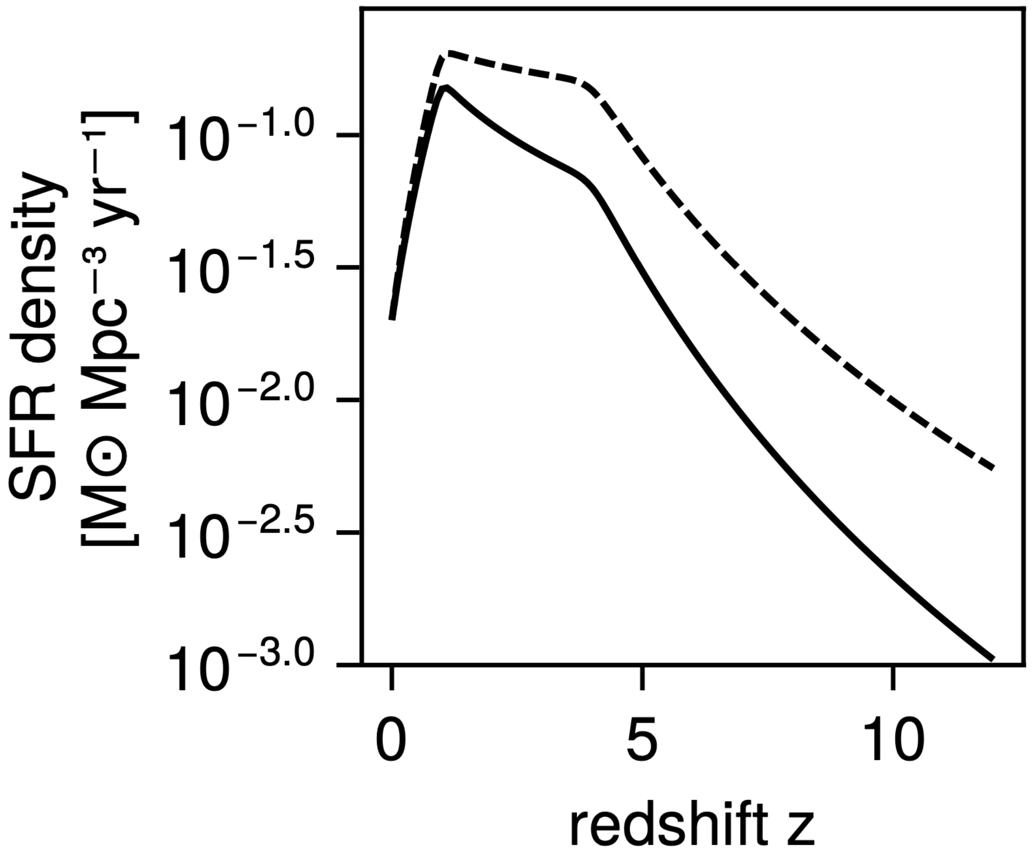

$$dN(z) \propto \dot{\rho}_\star(z) \times 4\pi D^2 \frac{dD}{dz} dz$$

with $D(z) = \int dz/H(z)$ the comoving distance.

SFRD model

---- YK08 —— EM20

Yuksel et al., 0804.4008 [astro-ph]
M. Elías-Chávez, O.M. Martínez, 2006.03367 [astro-ph.GA]

- We further assume that all sources emit identical fluxes.

$$\phi_\alpha = f_\alpha \phi_0 \left(\frac{E(1+z)}{E_0} \right)^{-\gamma}$$

(α is the flavor index)

Neutrino sources

- The flux contribution from the redshift interval $[z, z + dz]$ including Quasi-Dirac oscillations is given by

$$d\Phi_\beta(z, E) = \sum_\alpha P_{\alpha\beta}(z, E)\phi_\alpha(z, E)dN(z)\,.$$

- The total flux at Earth as function of energy is therefore

$$\Phi_\beta(E) \propto \int \sum_\alpha P_{\alpha\beta}(z, E) \times \dot{\rho}_\star(z) \times f_\alpha \phi^0 \left(\frac{E(1+z)}{E_0}\right)^{-\gamma} \frac{dz}{H(z)}\,.$$

SFRD model **spectral index**

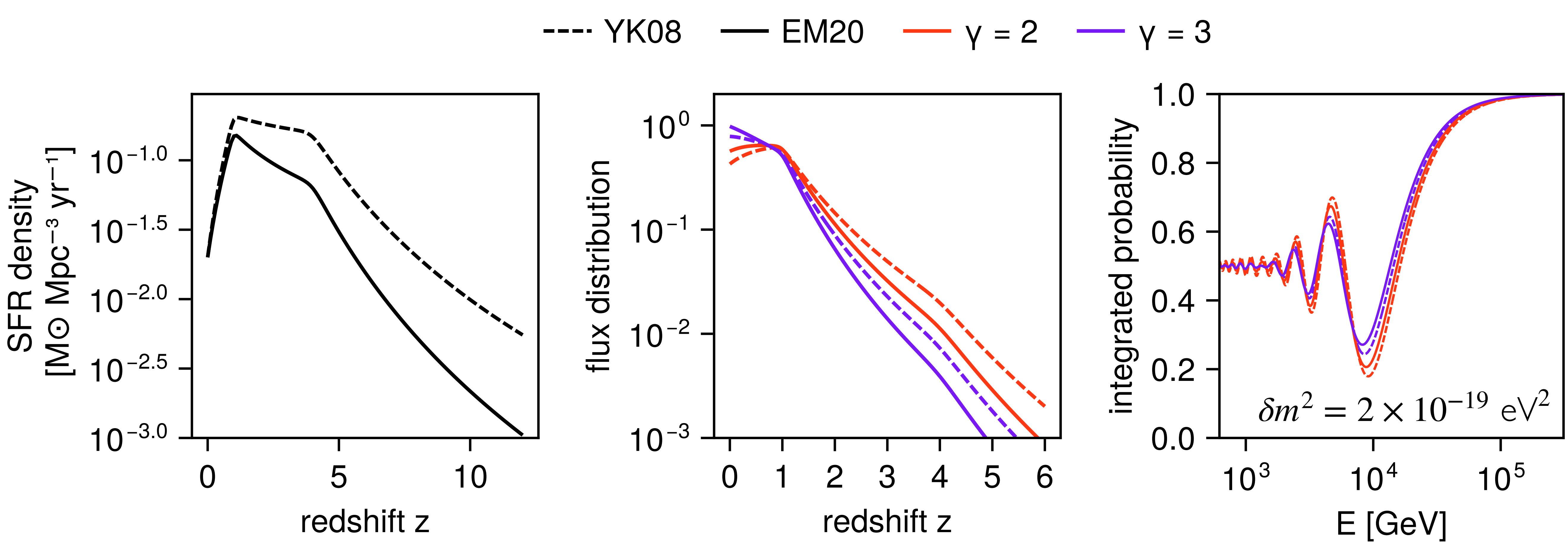

Results

Spectral features of Quasi-Dirac neutrinos

- Quasi-Dirac oscillations introduce spectral features in the diffuse flux, improving the fit to combined CASCADE and ESTES data, under the assumption that the astrophysical flux follows a SPL.
- Assuming equal mass-squared splittings for the three generations ($\delta m_1^2 = \delta m_2^2 = \delta m_3^2 = \delta m^2$), the best-fit value is $\delta m^2 = 1.91 \times 10^{-19}$ eV^2, yielding a fit improvement of $\Delta\chi^2 = 8.06$ (2.83σ).

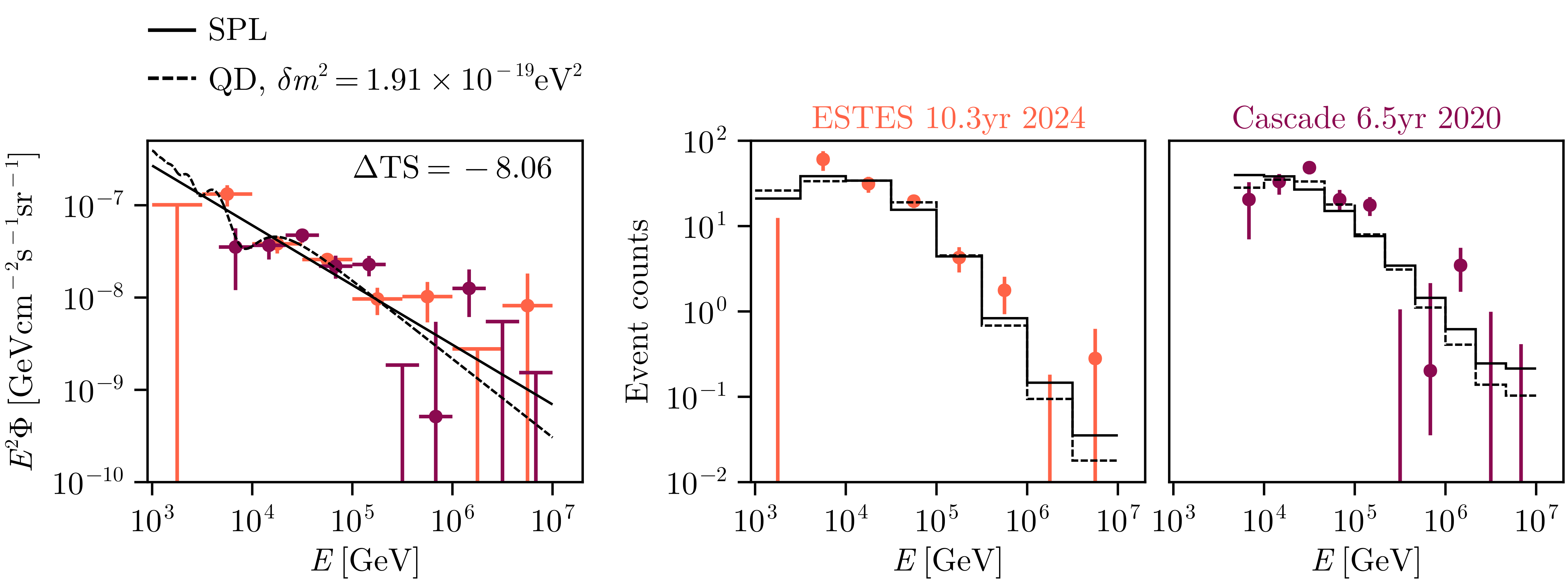

Preference for Quasi-Dirac neutrinos

- The larger preference, at the smaller δm^2, is driven by the deficit in the CASCADE sample below 30 TeV compared to ESTES.

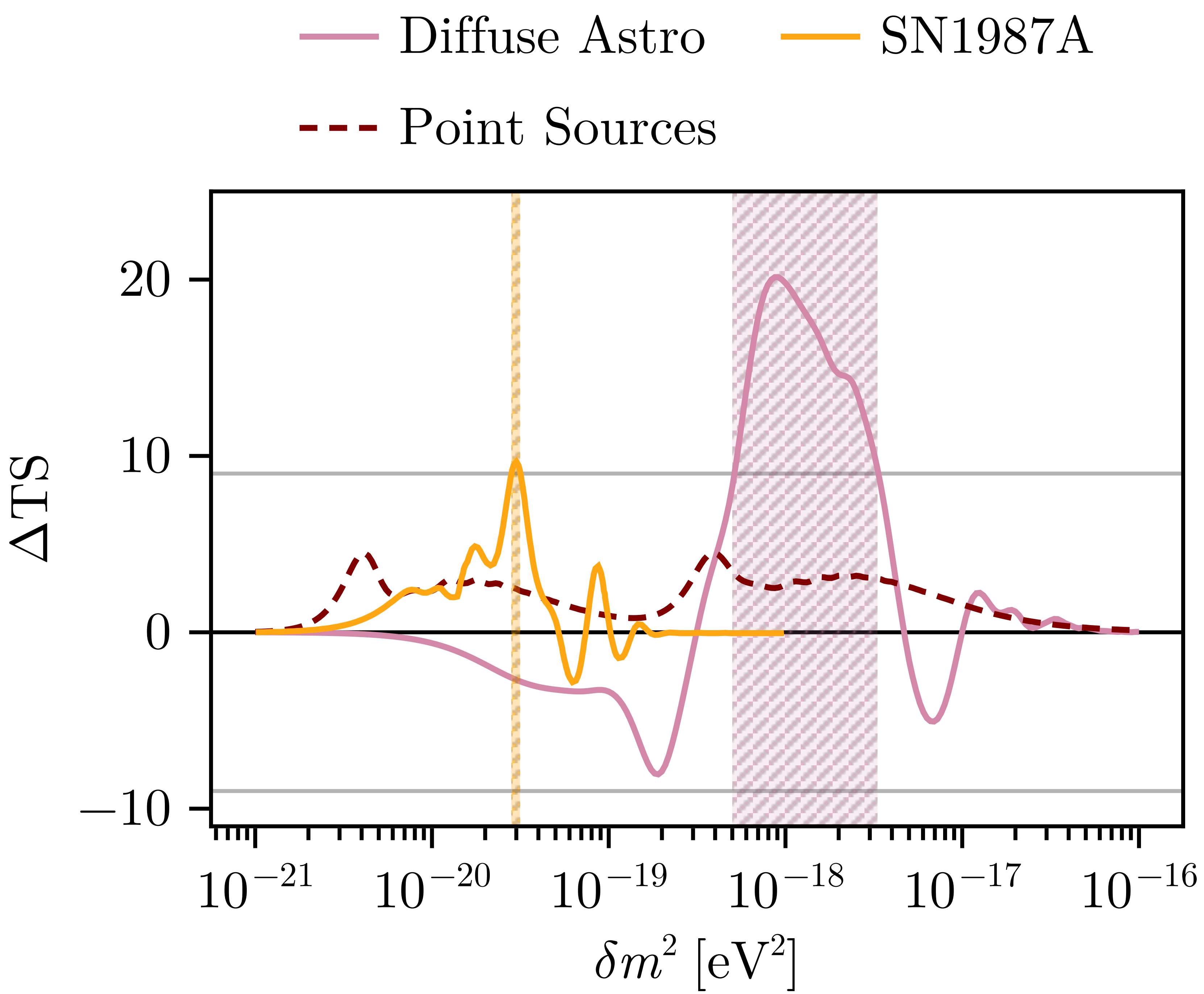

Preference for Quasi-Dirac neutrinos

- The smaller preference is caused by the lack of events in the `CASCADE` sample around 300 TeV.

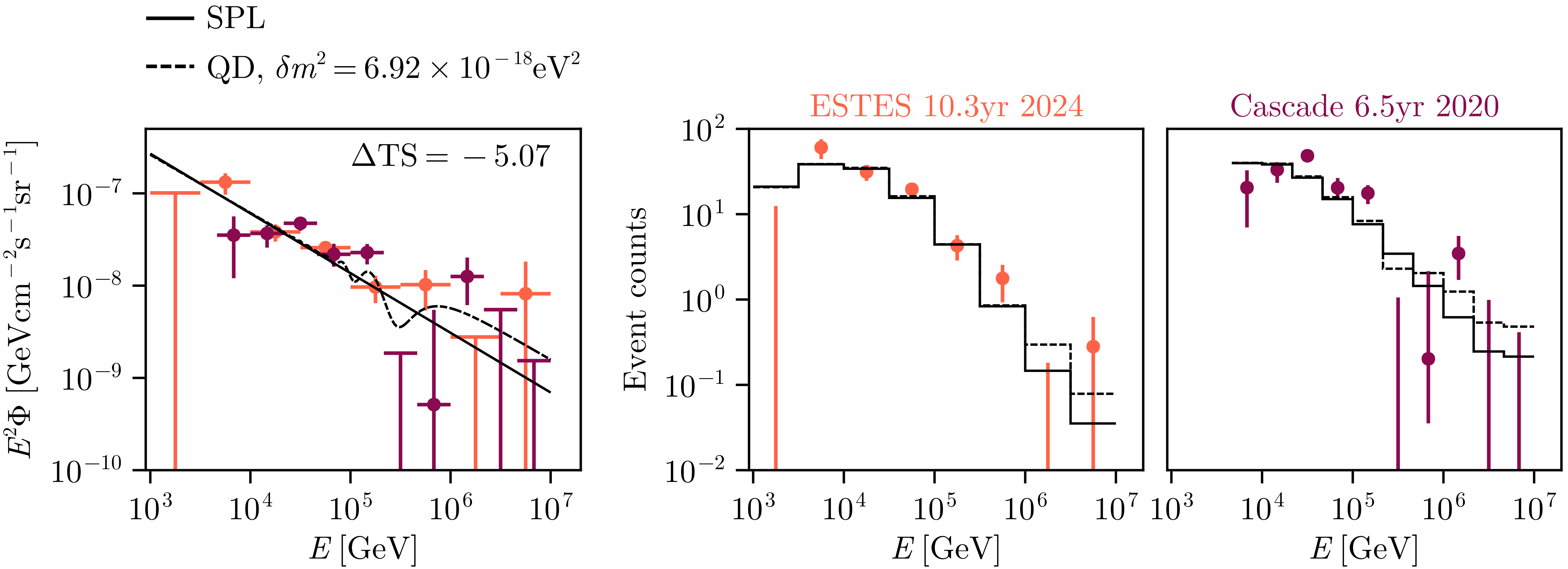

- Both preferences for a QD neutrinos are based on spectral effects only, which is possible because the two datasets report their results with different choices of energy binning.

Alternative source distributions

- The plot below shows the different astrophysical models for source distribution that we are currently testing.
- The lines in red are source populations that are relatively close to us and are disfavored from source searches, whereas the other ones are farther away.

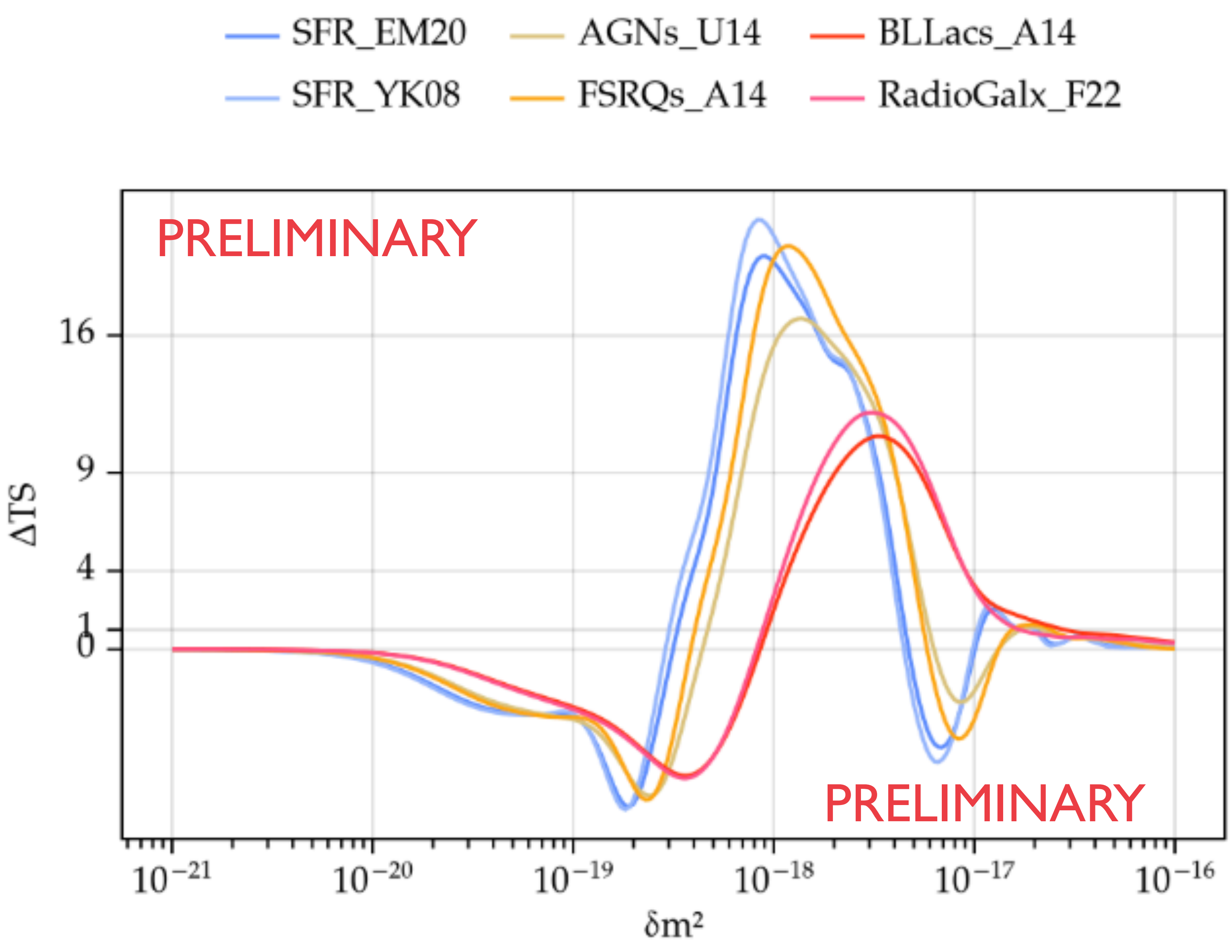

Conclusions

- QD neutrino oscillations lead to observable effects in the spectrum of astrophysical neutrinos.
- We use two IceCube event selections, CASCADE and ESTES, which have distinct flavor compositions, to probe the QD neutrinos parameter space.
- This new explanation of these spectral features is potentially testable in future observations of the diffuse flux or of point source spectra.

Conclusions

- QD neutrino oscillations lead to observable effects in the spectrum of astrophysical neutrinos.
- We use two IceCube event selections, CASCADE and ESTES, which have distinct flavor compositions, to probe the QD neutrinos parameter space.
- This new explanation of these spectral features is potentially testable in future observations of the diffuse flux or of point source spectra.

Thank you!

Backup Slides

Quasi-Dirac neutrinos

$\delta m_1^2[\mathrm{eV}^2]$	$\delta m_2^2[\mathrm{eV}^2]$	$\delta m_3^2[\mathrm{eV}^2]$	DOF	ΔTS
1.9×10^{-19}	δm_1^2	δm_1^2	1	-8.06
1.6×10^{-19}	2.0×10^{-19}	δm_2^2	2	-8.16
2.0×10^{-19}	2.0×10^{-19}	δm_1^2	2	-7.91
1.6×10^{-19}	δm_1^2	2.5×10^{-19}	2	-8.11

Quasi-Dirac neutrinos

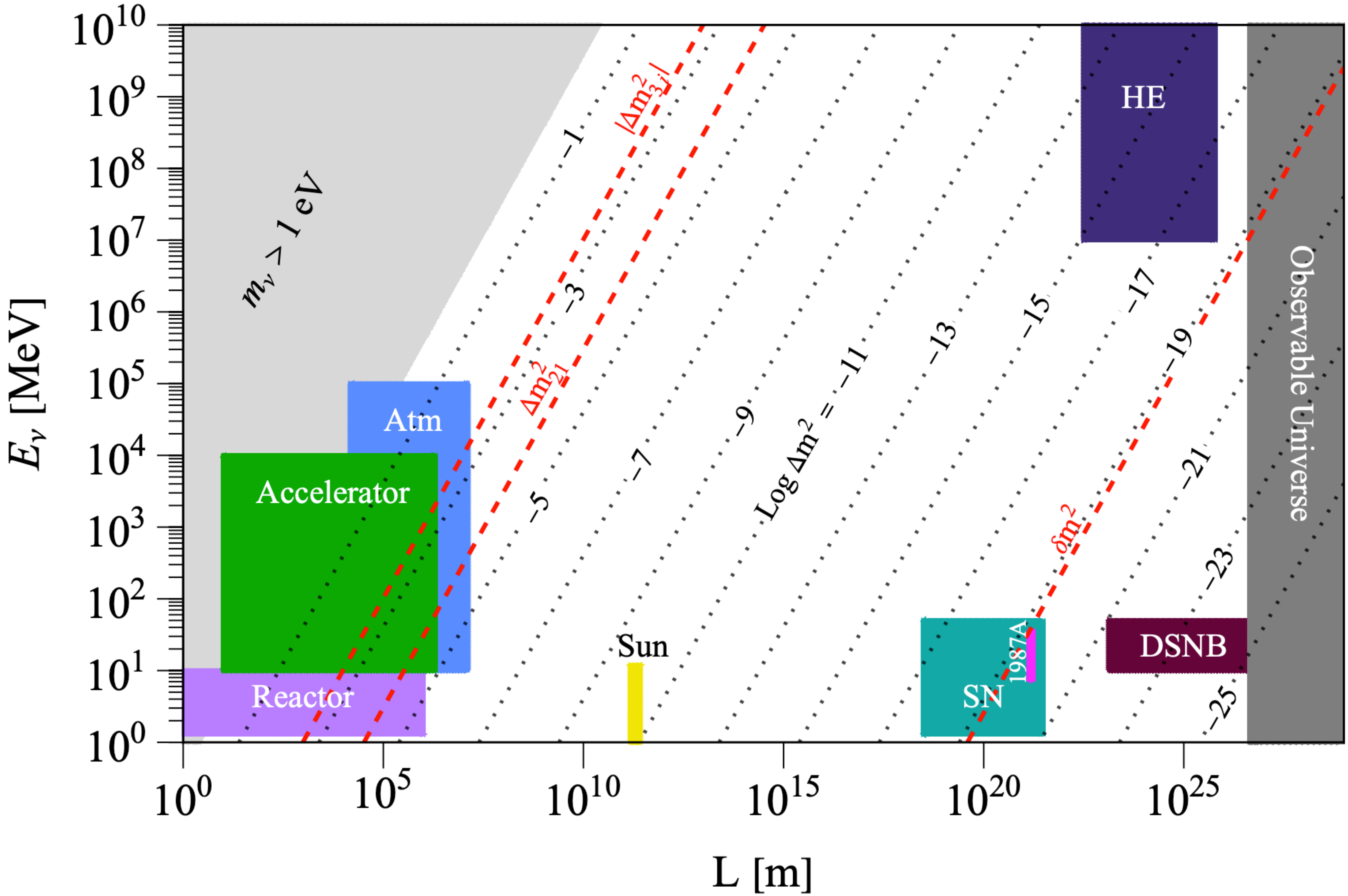

Martínez-Soler, Perez-Gonzales, Sen, arXiv:2105.12736 (PRD ’22)

Quasi-Dirac neutrinos improve the fit

Source Type	QD parameter(s)	Num. Parameters	$\Delta\chi^2$
Pion-decay	$\delta m_j^2 = \delta m^2$	1	8.06
Pion-decay	δm_1^2, $\delta m_2^2 = \delta m_3^2$	2	8.16
Pion-decay	δm_2^2, $\delta m_1^2 = \delta m_3^2$	2	7.91
Pion-decay	δm_3^2, $\delta m_1^2 = \delta m_2^2$	2	8.11

Quasi-Dirac neutrinos

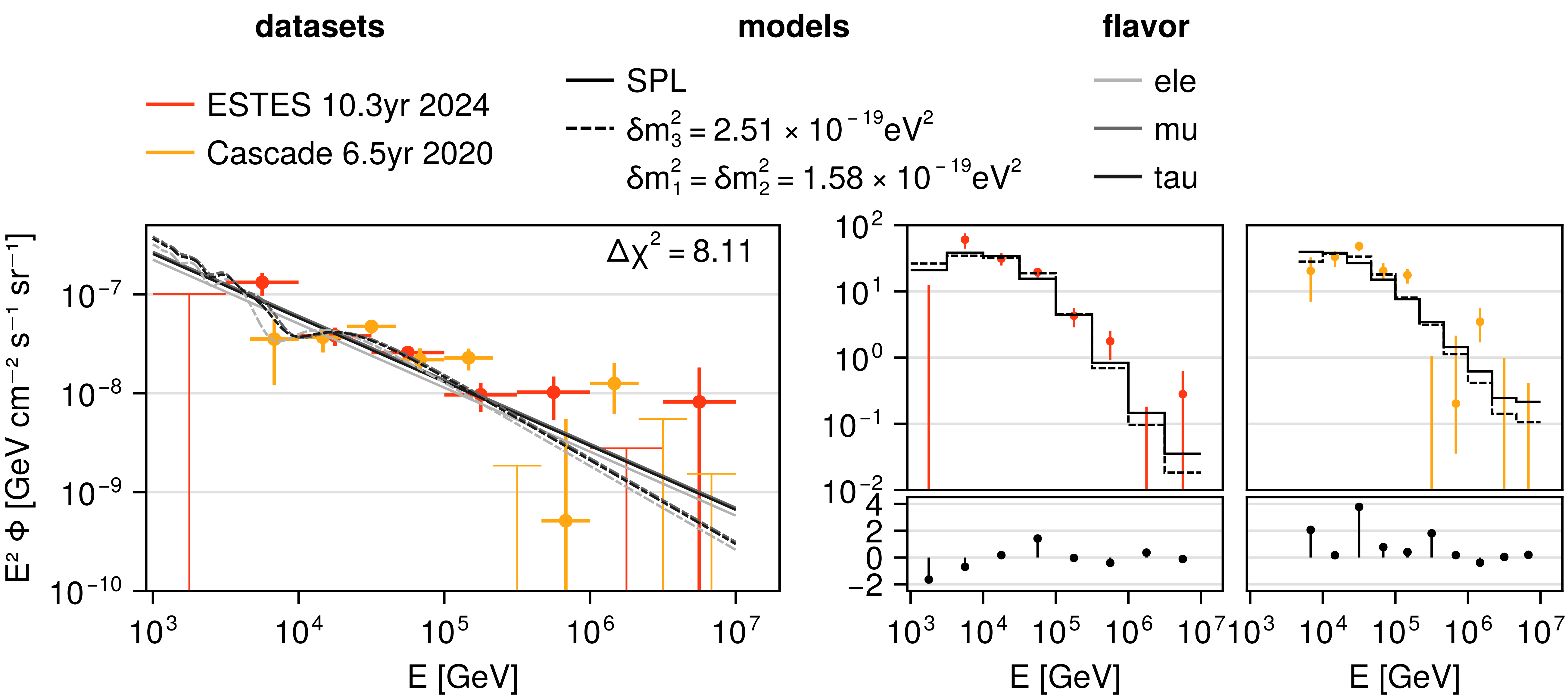

Coherence length

Note that, unlike standard oscillatory terms, quasi-Dirac oscillations are not necessarily washed out by extragalactic baselines. This is because the coherence length is

$$L_{\rm coh} = \frac{4\sqrt{2}E^2}{|\delta m_k^2|}\sigma_x$$
$$\approx 18~{\rm Gpc}\left(\frac{E}{10~{\rm TeV}}\right)^2\left(\frac{10^{-19}~{\rm eV}^2}{\delta m_k^2}\right)\left(\frac{\sigma_x}{10^{-19}~{\rm m}}\right).$$

Therefore, for benchmark values of 10 TeV and $\delta m_k^2 = 10^{-19}$ eV^2, the coherence length is comparable to the radius of the observable universe, even for the size of the wavepacket $\sigma_x \sim 10^{-19}$ m, orders of magnitude smaller than the smallest wave packets ever considered [71].

AGNs

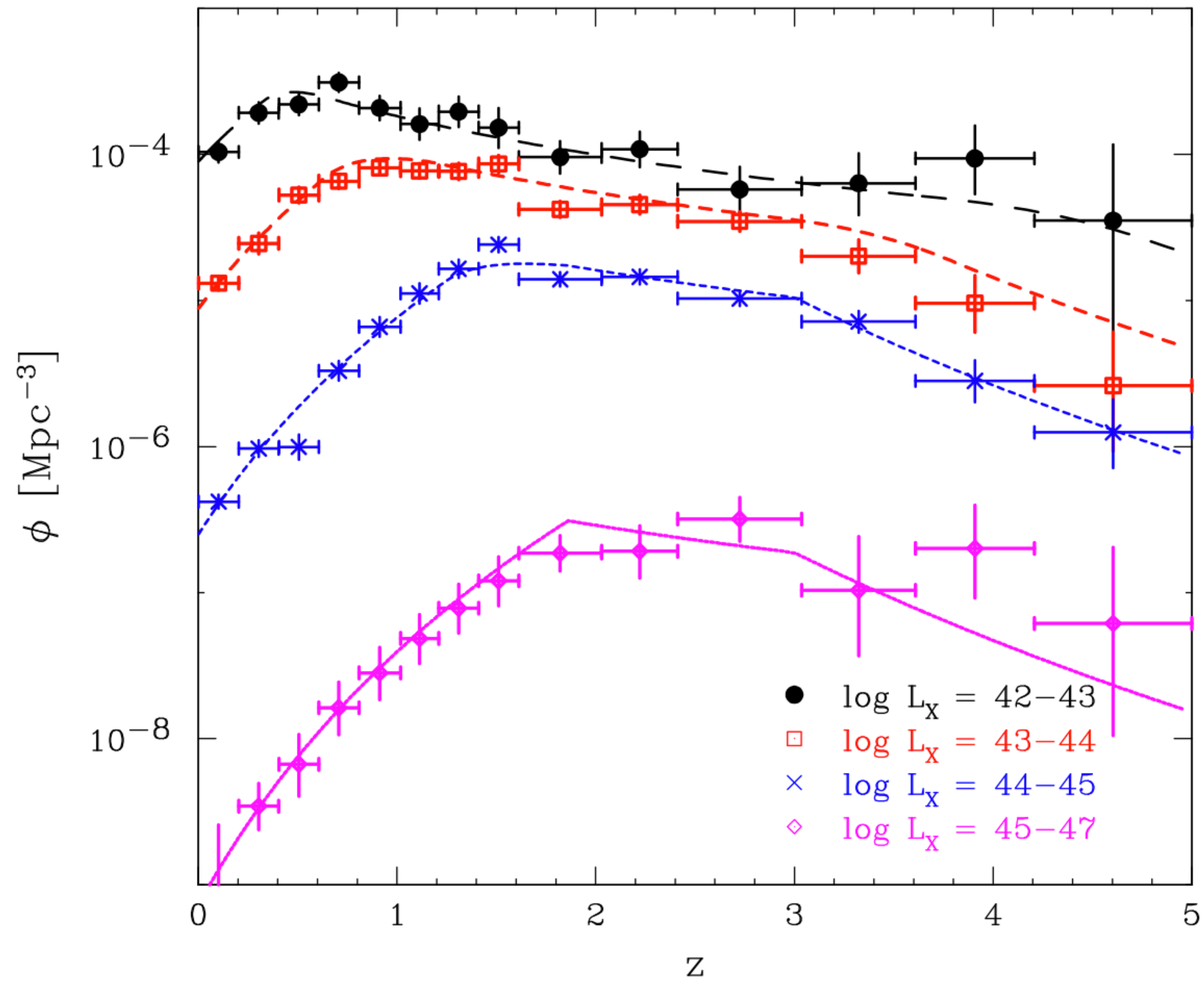

FIG. 12.— Comoving number density of AGNs plotted against redshift in different luminosity bins (CTN AGNs only). The curves are the best-fit model, and the data points are calculated from either the soft or hard band sample (see Section 6).

Leff

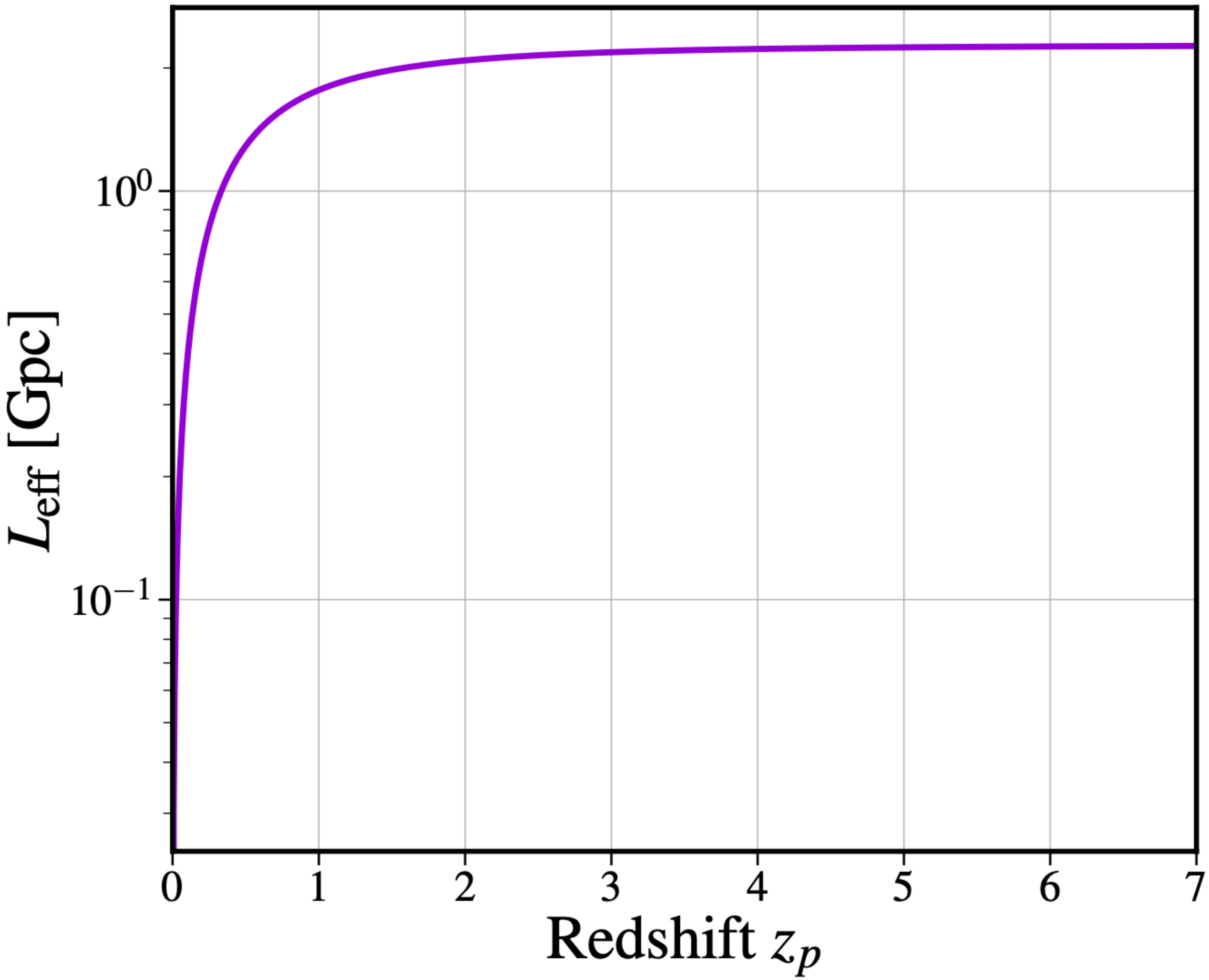

Leal et al., 2504.10576 [hep-ph]